



April, 1986

Forward Production of Heavy Flavours in Proton Nucleon Scattering¹

R. K. ELLIS

Fermi National Accelerator Laboratory
P.O. Box 500, Batavia, Illinois, 60510

Abstract

Lowest order QCD (gluon-gluon and quark anti-quark fusion in order α_s^2), predicts that heavy flavour production should fall off rapidly away from the central region. We calculate the process $g + q \rightarrow Q + \bar{Q} + q$ and present analytic results for the matrix element squared. This process is expected to give the dominant contribution in proton nucleon scattering along the direction of the incoming valence quark. After factorisation of the regions of collinear emission into the lowest order processes, the residual $O(\alpha_s^3)$ contribution has a small effect in the forward region. The production of heavy flavours calculated using perturbation theory is thus expected to be predominantly central. Other mechanisms, which may lead to non-central production of charmed quarks, are expected to fall off like a power of the heavy quark mass.

¹Talk presented at XXIIth Rencontre de Moriond, *Strong Interactions and Gauge Theories*, March 16-22, 1986, Les Arcs, Savoie, France

I. Introduction

It is common knowledge that perturbative QCD gives a poor description of the hadronic production of charmed particles at fixed target energies. For example, total cross-sections predicted by lowest order QCD lie below experimental results at fixed target energies, perhaps by more than an order of magnitude¹. Lowest order QCD also predicts predominantly central production of charmed hadrons, whereas experiments may indicate significant production in the forward region².

Before concluding that hadronic charm production is a failure of the theory, it is important to consider the mitigating circumstances. First and foremost it is questionable whether charm production is in fact described by perturbative QCD alone, because the mass of the charmed quark is not much heavier than the scale of the strong interactions. It should also be noted that experimental results are often based on a small number of events observed in a limited kinematic region. The estimation of total cross-sections from these results, requires large acceptance corrections, the size of which may depend sensitively on the model used. For data obtained from scattering on nuclear targets, comparison with theory requires an additional assumption about the atomic number dependence of the cross-sections.

It is also important to remember the imprecision of the perturbative QCD prediction itself. The 'standard' perturbative QCD formula for the inclusive charm production,

$$H(P_1) + H(P_2) \rightarrow Q(P_3) + X \quad (1.1)$$

is given by,

$$\frac{E_3 d\sigma}{d^3P_3} = \sum_{i,j} \int dx_1 dx_2 \left[\frac{E_3 d\hat{\sigma}_{ij}(\alpha_S(\mu^2), \hat{p}_1, \hat{p}_2)}{d^3P_3} \right]_{\hat{p}_1=x_1P_1, \hat{p}_2=x_2P_2} f_i(x_1, \mu^2) f_j(x_2, \mu^2) \quad (1.2)$$

The functions f are the distribution functions of light partons (gluons, light quarks and anti-quarks) evaluated at a scale μ , which is of the order of the mass of the produced heavy quark. $\hat{\sigma}$ is the short distance cross-section from which the mass singularities have been factored in the normal way³. Since the sensitivity to collinear emission has been removed from the short-distance cross-section, $\hat{\sigma}$, it is calculable as a perturbation series in $\alpha_S(\mu^2)$. The lowest order which contributes is $O(\alpha_S^2)$. In this order there are contributions to $\hat{\sigma}$ due to gluon gluon fusion and quark anti-quark annihilation. At fixed target energies the lowest order perturbative predictions, obtained using Eq.(1.2), depend sensitively on the input parameters, most notably the mass of the charmed quark. For example, at $\sqrt{S}=27$ GeV, we find that the total cross-section changes by more than an order of magnitude as we vary the mass of the charmed quark between 1.2 and 1.8 GeV. Such uncertainties also afflict the predictions for the longitudinal momentum distributions of the charmed quark.

In addition to the standard formula, Eq.(1.2), it has been suggested in the literature that the following mechanisms might contribute significantly to charmed particle production.

1. Flavour excitation graphs which contribute because of the presence of charmed quarks in the wave function of the incoming hadrons. The charmed quark content of the nucleon can be calculated using perturbation theory^{4,5,6]} or may be due to non-perturbative mechanisms, in which case it is said to be intrinsic^{7]}.
2. Diffractive production of a charmed quark pair from a gluon in one of the hadrons^{6,8]}.
3. Recombination of a produced charmed quark with a fast quark in one of the beam jets^{6]}.
4. Final state pre-binding distortion caused by the binding of charmed quarks to light quarks^{9]}.

The question which we wish to address in this paper is whether or not heavy flavours (bottom, top, etc.) will be copiously produced in the forward direction. This issue is relevant not only for present experiments but also for the design of detectors for future hadron colliders. All arguments presented here will be based on perturbation theory. Thus, strictly speaking we are considering the production of a heavy flavour, whose mass is very much bigger than the strong interaction scale ($m \gg \Lambda$). Examination of the dangerous regions of phase space in low order QCD diagrams indicates that the additional mechanisms enumerated above are **not** relevant for the production of very massive quarks^{10,11]}. They are either already included in the standard factorisation formula or suppressed by at least a power of the heavy quark mass. A definite confirmation of the validity of Eq.(1.2) for heavy quark production will require an all-orders proof, but the arguments of Collins, Soper and Sterman^{11]} make it plausible that the QCD improved parton model provides a reliable description of the hadronic production of heavy quarks. We therefore expect that the factorisation formula, Eq.(1.2) will be useful if we can neglect terms of order Λ/m where Λ is the QCD scale and m is the heavy quark mass. From a practical point of view it is also necessary to require that $\ln(m/\Lambda) \gg 1$, so that the hard scattering cross-section is accurately represented by a limited number of terms in its perturbative expansion.

The crucial issue is whether the charmed quark is massive enough to be considered a heavy quark in the sense described above. The charm quark mass lies in the range $m = 1.2 - 1.8$ GeV so it is obviously a borderline case. A full answer to the question of whether the charmed quark can be considered a heavy quark requires theoretical control of the terms which vanish as a power of m as well as the perturbative corrections, (the calculation of which is initiated here), which only vanish as a logarithm of the mass. No definitive answer to this question can be given here.

In this paper we use perturbation theory in order g^6 to calculate heavy quark production using the standard formula Eq.(1.2). We consider the process

$$g + q \rightarrow Q + \bar{Q} + q \tag{1.3}$$

The theoretical interest of this subprocess stems from the fact that it can be viewed as ‘containing’ both the flavour excitation of a heavy quark and the diffractive production of a heavy quark pair as subgraphs. The explicit calculation carried out here indicates that flavour excitation does not contribute in this order in perturbation theory. We find that the only singular regions correspond to the quark anti-quark and gluon-gluon fusion mechanisms. Our work can thus be regarded as a confirmation of the arguments of ref.(11). From a more practical point of view the higher order corrections provide theoretical information on the best choice of factorisation and renormalisation scale. The motivation for considering process of Eq.(1.3) (without considering all the other processes of order g^6) is that this process is expected to give the dominant contribution in the forward region in pN collisions. This is a consequence of the stiffness of the valence quark distribution in the proton in comparison with the anti-quark or gluon distributions. A priori, we expect that when $(1 - x_F) \simeq \alpha_S$ the process of Eq.(1.3) will be competitive with the lowest order process.

In Section (IV) we present numerical results for charmed quark production in the forward region. This is not because we can demonstrate that perturbation theory, (neglecting terms which vanish as a power of the charmed quark mass), gives a reliable prediction for charmed particle production in the forward region. It is rather our intention to make the perturbative prediction as precise as possible, in order to assess the significance of charmed particle production in the forward region.

II. Heavy Flavour Production in Lowest Order

The lowest order processes which contribute to the production of a heavy quark Q are the so-called fusion processes,

$$\begin{aligned} (a) \quad q(p_1) + \bar{q}(p_2) &\rightarrow Q(p_3) + \bar{Q}(p_4) \\ (b) \quad g(p_1) + g(p_2) &\rightarrow Q(p_3) + \bar{Q}(p_4) \end{aligned} \tag{2.1}$$

The four momenta of the partons are given in brackets. These processes have been thoroughly investigated in refs.[4,12,13]. However in order to regulate mass singularities we will need the forms of these matrix elements in $n = 4 - 2\epsilon$ dimensions¹⁴. We have therefore repeated the calculation of these matrix elements.

The Feynman diagram for quark anti-quark annihilation is shown in Fig. 1.

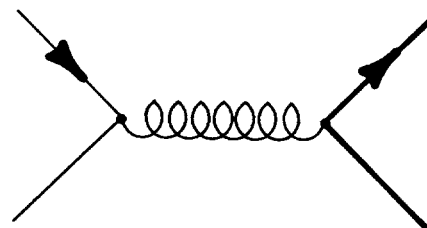


Figure 1: Lowest order diagram for the process $q + \bar{q} \rightarrow Q + \bar{Q}$.

The result for the matrix element squared, summed (averaged) over final (initial) colours and

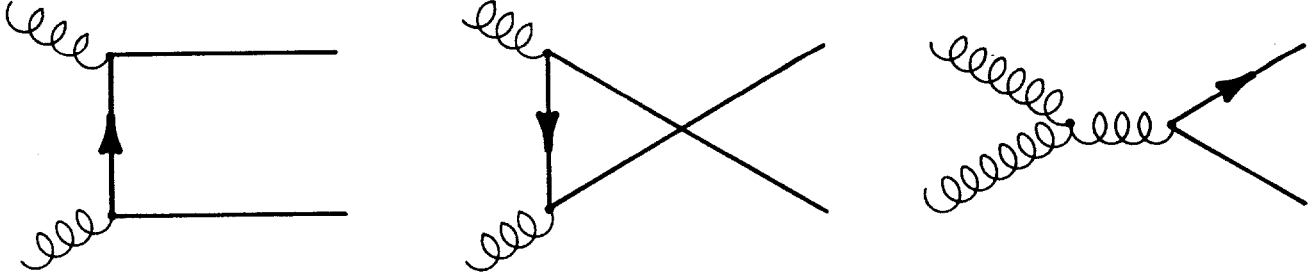


Figure 2: Lowest order diagrams for the process $g + g \rightarrow Q + \bar{Q}$.

spins can be expressed in terms of the transition probability $T_{\bar{q}q}$,

$$\begin{aligned} \overline{|M^{(a)}|^2} &= g^4 \mu^{4\epsilon} T_{\bar{q}q}(\tau_1, \tau_2, \rho, \epsilon) \\ T_{\bar{q}q}(\tau_1, \tau_2, \rho, \epsilon) &= \frac{V}{2N^2} \left(\tau_1^2 + \tau_2^2 + \frac{1}{2}\rho - \epsilon \right) \end{aligned} \quad (2.2)$$

where the dependence on the $SU(N)$ colour group is shown explicitly, ($V = N^2 - 1$, $N = 3$). Because this transition probability will ultimately be inserted in a QCD improved parton model formula we have chosen to express it in terms of variables which have simple behaviour under rescaling of the incoming momenta p_1 and p_2 .

$$\tau_1 = \frac{m^2 - t}{s} = \frac{p_1 \cdot p_3}{p_1 \cdot p_2}, \quad \tau_2 = \frac{m^2 - u}{s} = \frac{p_2 \cdot p_3}{p_1 \cdot p_2}, \quad \rho = \frac{4m^2}{s} \quad (2.3)$$

and $s = (p_1 + p_2)^2$, $t = (p_1 - p_3)^2$ and $u = (p_2 - p_3)^2$.

The Feynman diagrams for the gluon-gluon fusion process are shown in Fig. 2. It is convenient to divide the result for the transition probability into two pieces,

$$\begin{aligned} \overline{|M^{(b)}|^2} &= g^4 \mu^{4\epsilon} T_{gg}(\tau_1, \tau_2, \rho, \epsilon) \\ T_{gg}(\tau_1, \tau_2, \rho, \epsilon) &= T_{gg}^{(1)}(\tau_1, \tau_2, \epsilon) + T_{gg}^{(2)}(\tau_1, \tau_2, \rho, \epsilon) \end{aligned} \quad (2.4)$$

As before these results have been averaged and summed over initial colours and spins. The average over the spin of the initial gluons has been performed by dividing by $n - 2 = 2(1 - \epsilon)$. This is in agreement with the normal convention used in the calculation of the two loop anomalous dimensions^{15,16,17}. The results are,

$$\begin{aligned} T_{gg}^{(1)}(\tau_1, \tau_2, \epsilon) &= \frac{1}{2VN(1-\epsilon)} \left(\frac{V}{\tau_1\tau_2} - 2N^2 \right) (\tau_1^2 + \tau_2^2 - \epsilon) \\ T_{gg}^{(2)}(\tau_1, \tau_2, \rho, \epsilon) &= \frac{1}{2VN(1-\epsilon)^2} \left(\frac{V}{\tau_1\tau_2} - 2N^2 \right) \left(\rho - \frac{\rho^2}{4\tau_1\tau_2} \right) \end{aligned} \quad (2.5)$$

In the limit $\epsilon \rightarrow 0$ the factorised form in Eqs.(2.4, 2.5) agrees with the more complicated expression given in ref.(4).

The one parton inclusive cross-sections are determined by the transition probabilities given above,

$$\frac{p_3^0}{d^{n-1}p_3} d\sigma_{ij} = \mathcal{N} \frac{\alpha_S^2}{s^2} T_{ij}(\tau_1, \tau_2, \rho, \epsilon) \delta(1 - \tau_1 - \tau_2) \quad (2.6)$$

\mathcal{N} is an overall normalisation factor which is equal to one in four dimensions. Using the expression for the parton cross section given in Eq.(2.6), the QCD prediction for the process,

$$H(P_1) + H(P_2) \rightarrow Q(P_3) + X \quad (2.7)$$

can be cast in the characteristic parton model form,

$$\frac{E_3}{d^{n-1}P_3} d\sigma = \frac{\mathcal{N} \alpha_S^2(\mu^2)}{S^2} \sum_{i,j} \int \frac{dx_1}{x_1^2} \frac{dx_2}{x_2^2} f_i(x_1, \mu^2) f_j(x_2, \mu^2) T_{ij}(\tau_1, \tau_2, \rho, \epsilon) \delta(1 - \tau_1 - \tau_2) \quad (2.8)$$

In this equation the parton variables are expressed in terms of their hadronic counterparts as follows,

$$\tau_1 = \tau_1^H/x_2, \quad \tau_2 = \tau_2^H/x_1, \quad \rho = \rho^H/(x_1 x_2) \quad (2.9)$$

where,

$$\tau_1^H = \frac{P_1 \cdot P_3}{P_1 \cdot P_2}, \quad \tau_2^H = \frac{P_2 \cdot P_3}{P_1 \cdot P_2}, \quad \rho^H = \frac{4m^2}{S}, \quad S = (P_1 + P_2)^2 \quad (2.10)$$

The phenomenological implications of these lowest order estimates for the short distance cross-sections have been investigated elsewhere in the literature⁴. We list the salient features here,

1. They predict cross-sections which are predominantly central.
2. The rate of fall-off away from the central region is controlled by the stiffness of the distributions of gluons and light (anti-) quarks in the incoming hadrons.
3. The average transverse momentum of the heavy quarks is of the order of the mass of the produced heavy quark and the net transverse momentum of the pair of heavy quarks is small.

Parenthetically, we note that the number of charmed particles present in a jet has also been the subject of both experimental and theoretical analysis. As explained above the lowest order diagrams are not expected to contribute significantly in the region $p_T \gg m$. In this region, charmed particles are much more likely to be the fragmentation products of a gluon jet which is produced by the normal scattering between light partons. The higher order correction calculated in this paper can also be viewed as a contribution to this process.

$$g + q \rightarrow g + q \quad (2.11)$$

$$\quad \quad \quad \downarrow$$

$$\quad \quad \quad Q + \bar{Q}$$

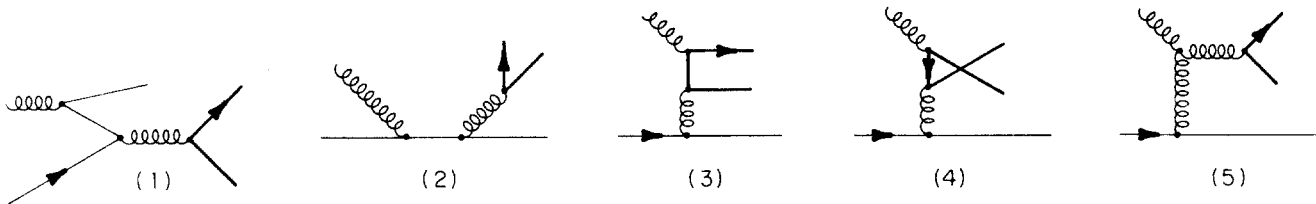


Figure 3: Diagrams of order g^3 which contribute to the process $g + q \rightarrow Q + \bar{Q} + q$.

Detailed results for the multiplicity of heavy quarks in a gluon jet have been given in ref.(18,19). Ref.(18) also includes estimates of the first non-perturbative contribution to gluon fragmentation into a heavy quark anti-quark pair. Although the presence of heavy flavours in jets may be of great experimental interest we do not consider this kinematic region further. We rather concentrate on the bulk of the cross-section which is produced at smaller transverse momenta of the order of the heavy quark mass.

III. Higher Order Corrections To Heavy Flavour Production

In order g^6 there are three types of process which contribute to the inclusive production of a heavy quark,

$$\begin{aligned}
 (A) \quad & q(p_1) + \bar{q}(p_2) \rightarrow Q(p_3) + X \\
 (B) \quad & g(p_1) + g(p_2) \rightarrow Q(p_3) + X \\
 (C) \quad & g(p_1) + q(p_2) \rightarrow Q(p_3) + X
 \end{aligned}
 \tag{3.1}$$

Processes *A* and *B* are radiative corrections to processes *a* and *b* in Eq. (2.1). A calculation of the order g^6 contributions of these processes would provide valuable information about the optimum choice for the scale μ . This information would be of phenomenological importance especially for charm production. In order g^6 the processes of Eq.(2.1) receive both real and virtual corrections which separately contain both soft and collinear singularities. The calculation of these radiative corrections remains an open and challenging problem.

The calculation of process *C* is much simpler since this process first appears at order g^6 . In order g^6 perturbation theory the relevant parton process is,

$$g(p_1) + q(p_2) \rightarrow Q(p_3) + \bar{Q}(p_4) + q(p_5), \quad p_3^2 = p_4^2 = m^2
 \tag{3.2}$$

The Feynman graphs which contribute to this process are shown in Fig. 3. We have calculated the full result for the matrix element in n dimensions averaged and summed over initial and

final colours and spins. The result is denoted by C .

$$\overline{\sum} |M^{(C)}|^2 = g^6 \mu^{6\epsilon} C(p_1, p_2, p_3, p_4, p_5) \quad (3.3)$$

By examination of the graphs of Figure 3, we see that graph 1 contains a mass singularity which can be identified as a contribution to the quark anti-quark fusion process of Eq.(2.1). In a similar way diagrams 3, 4 and 5 contain singularities which contribute to the gluon-gluon fusion process. Of course it is only in a physical gauge that the mass singularities be ascribed to particular diagrams in this way. Our first step is to isolate the contribution of these singular regions in the matrix element squared C , calculated using the full gauge invariant set of diagrams given in Fig.3. In the limit $p_1.p_5 \rightarrow 0$, the full n dimensional matrix element becomes,

$$C(p_1, p_2, p_3, p_4, p_5) \rightarrow C^{[15]}(p_1, p_2, p_3, p_4, p_5) = \frac{1}{p_1.p_5} \left[T_{\bar{q}q}(\tau_1, 1 - \tau_1, \frac{\rho}{z_1}, \epsilon) \frac{1}{z_1} P_{\bar{q}g}(z_1, \epsilon) \right] \quad (3.4)$$

$P_{\bar{q}g}$ is the splitting kernel^[20] in n dimensions and describes the perturbative probability of finding an anti-quark in the incoming gluon,

$$P_{\bar{q}g}(z, \epsilon) = \frac{T_R}{1 - \epsilon} (z^2 + (1 - z)^2 - \epsilon), \quad z_1 = \frac{\tau_2}{1 - \tau_1}, \quad T_R = \frac{1}{2} \quad (3.5)$$

In order to investigate the limit $p_2.p_5 \rightarrow 0$, it is convenient to move to the centre of mass system of the $\bar{Q}q$ system ($\vec{p}_4 + \vec{p}_5 = 0$). In this frame we may write,

$$p_4 = \frac{(s_{45} + m^2)}{2\sqrt{s_{45}}} (1, \dots, -\lambda \sin \theta_1 \cos \theta_2, -\lambda \cos \theta_1), \quad \lambda = \frac{s_{45} - m^2}{s_{45} + m^2} \quad (3.6)$$

$$p_5 = \frac{(s_{45} - m^2)}{2\sqrt{s_{45}}} (1, \dots, \sin \theta_1 \cos \theta_2, \cos \theta_1)$$

In Eq.(3.6) the dots represent $n - 3$ components of momenta which are determined by the mass-shell conditions $p_4^2 = m^2$, $p_5^2 = 0$. We have introduced the notation, $s_{45} = (p_4 + p_5)^2$. In the same system we may choose,

$$p_1 = \frac{(s_{45} - u)}{2\sqrt{s_{45}}} (1, \dots, \sin \alpha, \cos \alpha) \quad (3.7)$$

$$p_2 = \frac{(s_{45} - t)}{2\sqrt{s_{45}}} (1, \dots, 0, 1)$$

In Eq.(3.7) the dots represent $n - 3$ zero momentum components. p_3 is determined by overall energy-momentum conservation. The limit $p_2.p_5 \rightarrow 0$ corresponds to the region of collinear

emission from the incoming quark with momentum p_2 , ($\theta_1 \rightarrow 0$). In this limit we obtain,

$$\begin{aligned}
C(p_1, p_2, p_3, p_4, p_5) &\rightarrow \\
C^{[25]}(p_1, p_2, p_3, p_4, p_5) &= \frac{1}{p_2 \cdot p_5} \left[T_{gg}(1 - \tau_2, \tau_2, \frac{\rho}{z_2}, \epsilon) \frac{1}{z_2} P_{gq}(z_2, \epsilon) \right. \\
&\quad \left. + T_{gg}^{(2)}(1 - \tau_2, \tau_2, \frac{\rho}{z_2}, \epsilon) \left(2(1 - \epsilon) \cos^2 \theta_2 - 1 \right) \frac{V}{N} \frac{1 - z_2}{z_2^2} \right]
\end{aligned} \tag{3.8}$$

where P_{gq} is the splitting function^{20]} in n dimensions.

$$P_{gq}(z, \epsilon) = \frac{V}{2N} \left(\frac{1 + (1 - z)^2 - \epsilon z^2}{z} \right), \quad z_2 = \frac{\tau_1}{1 - \tau_2} \tag{3.9}$$

Note that the second term in Eq.(3.8) vanishes after averaging over the angle θ_2 (even in n dimensions) to reproduce the expected factorisation result for the inclusive cross-section.

By now the strategy of the calculation should be clear. The difference

$$C(p_1, p_2, p_3, p_4, p_5) - C^{[15]}(p_1, p_2, p_3, p_4, p_5) - C^{[25]}(p_1, p_2, p_3, p_4, p_5) \tag{3.10}$$

is perfectly finite in all regions of phase space and hence the limit $n \rightarrow 4$ can be taken. The contribution of the difference Eq.(3.10) to the inclusive charm production cross-section will be evaluated by numerical integration. The limit $\epsilon \rightarrow 0$ of $C^{[15]}$ and $C^{[25]}$ can be obtained from Eqs.(3.4, 3.8).

In four dimensions, using the momentum assignments of Eq.(3.2), C becomes,

$$\begin{aligned}
& C(p_1, p_2, p_3, p_4, p_5) \rightarrow \\
& \left[\frac{2 \{23\}^2 + 2 \{24\}^2 + 2 \{35\}^2 + 2 \{45\}^2 + m^2(t_{25} + s_{34})}{2 t_{25} s_{34}} \right] \\
& \times \left[\frac{N^2 - 4}{4N^2} \right. \\
& \left(\frac{2 \{24\}}{\{12\}\{14\}} - \frac{2 \{23\}}{\{12\}\{13\}} + \frac{2 \{35\}}{\{13\}\{15\}} - \frac{2 \{45\}}{\{14\}\{15\}} - \frac{\{25\}}{\{12\}\{15\}} - \frac{\{34\}}{\{13\}\{14\}} \right) \\
& + \frac{1}{4} \left(\frac{\{25\}}{\{12\}\{15\}} + \frac{\{34\}}{\{13\}\{14\}} - \frac{2 \{23\}}{\{12\}\{13\}} - \frac{2 \{24\}}{\{12\}\{14\}} - \frac{2 \{35\}}{\{13\}\{15\}} - \frac{2 \{45\}}{\{14\}\{15\}} \right) \left. \right] \\
& + \frac{N^2 - 4}{N^2} \frac{m^2}{s_{34} t_{25}} \left[\frac{\{35\} + \{23\}}{\{14\}} - \frac{\{45\} + \{24\}}{\{13\}} \right] \\
& + \frac{V}{N^2} m^2 \left[\frac{1}{s_{34}^2} \left(\frac{\{12\}^2 + \{15\}^2}{\{12\}\{15\}} \right) + \frac{1}{2 s_{34}} \left(\frac{1}{\{12\}} - \frac{1}{\{15\}} - \frac{1}{\{13\}} - \frac{1}{\{14\}} \right) \right. \\
& + \frac{1}{2 t_{25}} \left(\frac{m^2}{\{13\}^2} + \frac{m^2}{\{14\}^2} - \frac{1}{\{13\}} - \frac{1}{\{14\}} + \frac{4}{s_{34}} \right) + \frac{\Delta_1^2 + \Delta_2^2 + \Delta_3^2 + \Delta_4^2}{t_{25}^2} \left. \right] \\
& + \frac{1}{N^2} \frac{m^2}{s_{34} t_{25}} \left[1 + \frac{t_{25}}{s_{34}} - \frac{m^2}{\{13\}} - \frac{m^2}{\{14\}} + \frac{\{12\}^2 + \{15\}^2}{\{13\}\{14\}} \right. \\
& \left. - 2 \left(\{24\} + \{45\} \right) \frac{(\Delta_1 + \Delta_2)}{t_{25}} - 2 \left(\{23\} + \{35\} \right) \frac{(\Delta_3 + \Delta_4)}{t_{25}} \right] \tag{3.11}
\end{aligned}$$

In this equation we have introduced the notation,

$$\begin{aligned}
s_{34} &= (p_3 + p_4)^2, \quad t_{25} = (p_2 - p_5)^2, \quad p_j \cdot p_k = \{jk\} \\
\Delta_1 &= \frac{p_2 \cdot p_4}{p_1 \cdot p_3} - \frac{2p_1 \cdot p_2}{s_{34}}, \quad \Delta_2 = \frac{p_4 \cdot p_5}{p_1 \cdot p_3} - \frac{2p_1 \cdot p_5}{s_{34}} \\
\Delta_3 &= \frac{p_2 \cdot p_3}{p_1 \cdot p_4} - \frac{2p_1 \cdot p_2}{s_{34}}, \quad \Delta_4 = \frac{p_3 \cdot p_5}{p_1 \cdot p_4} - \frac{2p_1 \cdot p_5}{s_{34}}
\end{aligned} \tag{3.12}$$

The differences $\Delta_1, \Delta_2, \Delta_3$ and Δ_4 vanish in the limit $t_{25} \rightarrow 0$ as a square root of t_{25} . This is sufficient to reduce all the apparent double poles of t_{25} in Eq.(3.11) to single poles. This result, which holds also in n dimensions, is already evident from the explicit result given in Eq.(3.8). In the limit $m = 0$, Eq.(3.11) is in agreement with ref.(21). Numerical results for this process including masses have been given in ref.(22). All analytic results were obtained using the algebraic manipulation program Schoonschip²³.

We must now evaluate the contribution to the cross-section of the subtraction terms $C^{[15]}$ and $C^{[25]}$. These pieces contain singularities and will be evaluated analytically in n dimen-

sions. The n dimensional phase space for the process in Eq.(3.2) can be cast in the form

$$(PS)^{(3)} = \frac{(2\pi)^{2\epsilon}}{2^7\pi^4} \int \frac{d^{n-1}p_3}{E_3} \int d\tau_{45} \delta(1 - \tau_1 - \tau_2 - \tau_{45}) \left(\frac{\tau_{45}}{\tau_{45} + \rho/4} \right) \left(\frac{\tau_{45} + \rho/4}{\tau_{45}^2} \right)^\epsilon \left(\frac{4\pi}{s} \right)^\epsilon \frac{\Gamma(1 - \epsilon)}{\Gamma(1 - 2\epsilon)} I \quad (3.13)$$

In this equation $n - 4$ irrelevant angles have been integrated over and $\tau_{45} = p_4 \cdot p_5 / p_1 \cdot p_2$. The dependence on the angles θ_1 and θ_2 , which are defined in the reference frame given in Eq.(3.6,3.7), is contained in I ,

$$I = \frac{1}{2\pi} \int_0^\pi d\theta_1 \sin^{1-2\epsilon} \theta_1 \int_0^\pi d\theta_2 \sin^{-2\epsilon} \theta_2 \quad (3.14)$$

After angular integration the contribution of $C^{[15]}$ and $C^{[25]}$ to the inclusive charm production cross-section at the parton level can be cast in the factorised form,

$$p_3^0 \frac{d^{n-1}\sigma_{ij}}{d^{n-1}p_3} = \sum_{i',j'} \int_0^1 dz_1 dz_2 \left[\left\{ p_3^0 \frac{d^{n-1}\hat{\sigma}_{i'j'}}{d^{n-1}p_3} \right\} \Gamma_{j'j}(z_2, \epsilon) \Gamma_{i'i}(z_1, \epsilon) \right] \quad (3.15)$$

where the short distance cross-section $\hat{\sigma}$ is evaluated at rescaled values of the parton-momenta,

$$\hat{p}_1 = z_1 p_1, \quad \hat{p}_2 = z_2 p_2, \quad (3.16)$$

For the particular gluon quark process which we are calculating Eq.(3.15) becomes,

$$p_3^0 \frac{d^{n-1}\sigma_{gq}}{d^{n-1}p_3} = \int_0^1 dz_1 \left[p_3^0 \frac{d^{n-1}\hat{\sigma}_{\bar{q}q}}{d^{n-1}p_3} \right] \Gamma_{\bar{q}g}(z_1, \epsilon) + \int_0^1 dz_2 \left[p_3^0 \frac{d^{n-1}\hat{\sigma}_{gg}}{d^{n-1}p_3} \right] \Gamma_{gq}(z_2, \epsilon) + \left[p_3^0 \frac{d^{n-1}\hat{\sigma}_{gg}}{d^{n-1}p_3} \right] + O(\alpha_S^4) \quad (3.17)$$

The singularities present in the subtraction terms $C^{[15]}$ and $C^{[25]}$ now appear as poles in ϵ in the functions Γ . To first order in α_S the singular parts of the functions Γ are given by the Altarelli-Parisi functions. At this order we may define the functions Γ to be,

$$\Gamma_{ii'}(z, \epsilon) = \delta_{ii'} \delta(1 - z) - \frac{\alpha_S}{2\pi} P_{ii'}(z, 0) \left(\frac{1}{\epsilon} + \ln(4\pi) - \gamma_E \right) \quad (3.18)$$

The association of the $\ln(4\pi)$ and Euler constant with the pole in ϵ defines this to be the \overline{MS} type of mass singularity factorisation²⁴. This is the factorisation scheme used everywhere in this paper. As indicated in the previous sections, the parton cross-sections σ are calculated by averaging over $n - 2$ spin states of initial gluons.

The short distance cross-sections $\hat{\sigma}_{\bar{q}q}$ and $\hat{\sigma}_{gg}$ are given at order α_S^2 by Eq.(2.6). The

residual term $\hat{\sigma}_{gq}$ is perfectly finite and we may take the limit $n \rightarrow 4$. In this limit we obtain,

$$\begin{aligned}
p_3^0 \frac{d^3 \hat{\sigma}_{gq}}{d^3 p_3} = & \\
\alpha_s^2 \frac{\alpha_S}{2\pi} \frac{1}{(1-\tau_1)} T_{\bar{q}q}(\tau_1, \tau_2/z_1, \rho/z_1) & \left[\frac{P_{\bar{q}g}(z_1, 0)}{z_1} Y + 2T_R(1-z_1) \right] \\
+ \alpha_s^2 \frac{\alpha_S}{2\pi} \frac{1}{(1-\tau_2)} T_{gg}(\tau_1/z_2, \tau_2, \rho/z_2) & \left[\frac{P_{gq}(z_2, 0)}{z_2} Y + \frac{V}{2N} \right]
\end{aligned} \tag{3.19}$$

where,

$$Y = \ln \left(\frac{(1-\tau_1-\tau_2)^2 s}{(1-\tau_1-\tau_2+\rho/4)\mu^2} \right), \quad z_1 = \frac{\tau_2}{1-\tau_1}, \quad z_2 = \frac{\tau_1}{1-\tau_2} \tag{3.20}$$

The full answer for the short distance cross-section $\hat{\sigma}_{gq}$ is obtained by adding the contribution of Eq.(3.19) to the numerically evaluated contribution coming from the finite difference Eq.(3.10).

Before presenting numerical results we make some remarks of a more theoretical nature. By explicit computation we have shown that the only singular contributions in the full matrix element for process C come from regions which can be associated with quark anti-quark annihilation and gluon-gluon fusion. In particular, in extracting the singular part of the full matrix element squared (Eq.(3.11) and its n dimensional generalisation) we found that the double poles in t_{25} vanish. The cancellation of the double poles can be simply demonstrated on a graph-by-graph basis working in the gauge $p_1 \cdot A = 0$. Naive power counting works in this gauge as long as the mass of the recoil system is greater than zero $(p_1 + p_2 - p_5)^2 \sim M^2 > 0$. This reduction of the double pole to a single pole has also been considered in ref.[11].

Had the double poles persisted in the full answer they would have emphasized the low momentum region in heavy quark production. This would have suggested that mechanisms not described by perturbation theory were important for heavy quark production. It would also have lead to large production in the forward region.

Even after the cancellation of the double poles, the remaining $1/t_{25}$ term still displays a logarithmic sensitivity to the low momentum region. This sensitivity is the familiar one due to collinear parton emission and is removed by factoring the low momentum region $|t_{25}| < \mu^2$, $|t_{15}| < \mu^2$ into the incoming hadron wave-functions. In the remaining cross-sections all propagators are off-shell by at least $\mu^2 \sim m^2$. It is hence a bona fide higher order term in the short distance cross-section. There is no room left for a flavour excitation contribution.

IV. Numerical Results

In this section we present numerical results for charm production cross-sections using the standard parton model formula Eq.(1.2). We have used the parton distribution functions of

Table 1: Total cross-sections for the production of charmed quarks under various assumptions for the input parameters.

	$\sigma_{gg} (\mu b)$	$\sigma_{q\bar{q}} (\mu b)$	$\sigma_{TOT} (\mu b)$
$\sqrt{S} = 27.0 \text{ GeV}, pp$			
DO1, $\Lambda=0.2 \text{ GeV}, m=1.8 \text{ GeV}$	1.2	0.16	1.3
DO2, $\Lambda=0.4 \text{ GeV}, m=1.2 \text{ GeV}$	17.	2.7	19.7
DO2, $\Lambda=0.4 \text{ GeV}, m=1.2 \text{ GeV}, m_{th}= 1.8 \text{ GeV}$	9.0	.7	9.7
$\sqrt{S} = 62.4 \text{ GeV}, pp$			
DO1, $\Lambda=0.2 \text{ GeV}, m=1.8 \text{ GeV}$	7.6	0.7	8.3
DO2, $\Lambda=0.4 \text{ GeV}, m=1.2 \text{ GeV}$	42.3	8.1	50.4
DO2, $\Lambda=0.4 \text{ GeV}, m=1.2 \text{ GeV}, m_{th}= 1.8 \text{ GeV}$	26.7	3.0	29.8
$\sqrt{S} = 630. \text{ GeV}, p\bar{p}$			
DO1, $\Lambda=0.2 \text{ GeV}, m=1.8 \text{ GeV}$	85.	4.0	89.
DO2, $\Lambda=0.4 \text{ GeV}, m=1.2 \text{ GeV}$	169.	31.7	200.
DO2, $\Lambda=0.4 \text{ GeV}, m=1.2 \text{ GeV}, m_{th}= 1.8 \text{ GeV}$	117.	15.5	132.5

Duke and Owens^{25]}. These exist in two versions.

1. soft gluon distributions, $\Lambda=0.2 \text{ GeV}$, (DO1).
2. hard gluon distributions, $\Lambda=0.4 \text{ GeV}$, (DO2).

As a preliminary test we have investigated the sensitivity of the total charm production cross-section to variations in the input parameters. From Table 1 we see that the cross-sections depend sensitively on the charm quark mass. Because of smaller quark anti-quark luminosity it contributes only about 10% of the cross-section in proton-nucleon collisions. In calculating the total cross-section with a light quark mass ($m=1.2 \text{ GeV}$) we have also investigated the effect of imposing a physical threshold ($s > 4m_{th}^2$). The resultant total cross-sections are shown in Table I at $\sqrt{S}=27.0 \text{ GeV}$, $\sqrt{S}=62.4 \text{ GeV}$ and $\sqrt{S}=630.0 \text{ GeV}$. Near threshold there is a considerable sensitivity to the value of the heavy quark mass which provides the hard scale for the interaction. These large variations in the total cross-sections should be borne in mind when looking at the more differential distributions which follow. At collider energies the sensitivity to the heavy quark mass is reduced, but the parton luminosities are uncertain because the value of $x \approx 2m/\sqrt{S}$ is so small.

The Feynman x_F distribution coming from the lowest order gluon gluon fusion and quark anti-quark annihilation are shown in Fig. 4. The cross-section falls steeply with x_F ; by $x_F = 0.5$ it has fallen by about two orders of magnitude from its central value. Fig. 5 displays the result of including the higher order correction calculated in Section III. Numerical results were obtained using the adaptive Monte Carlo integration program Vegas^{26]}. We have set the

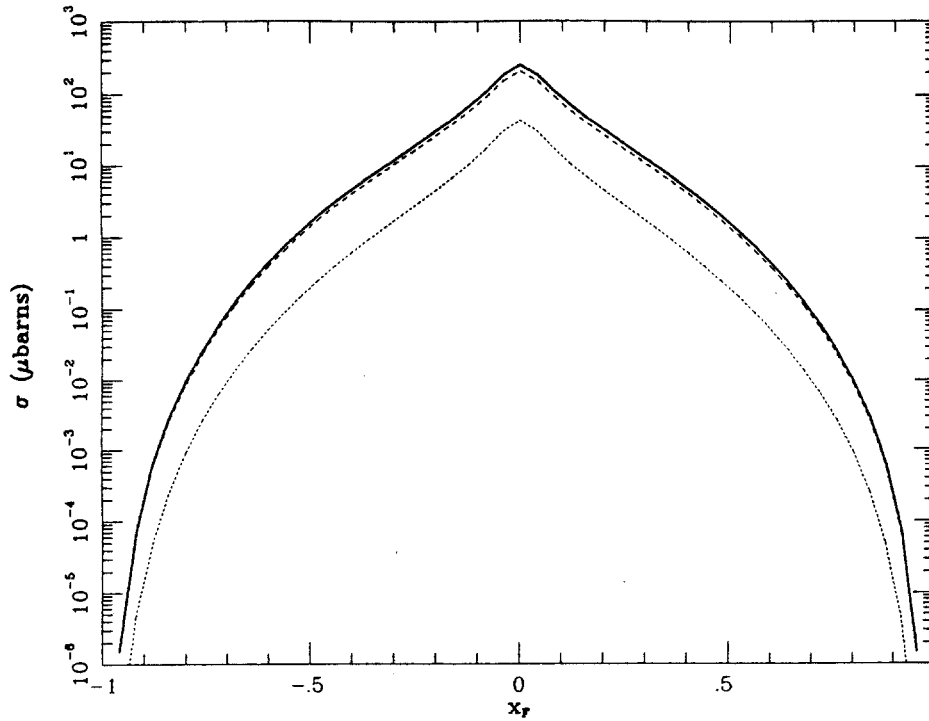


Figure 4: The differential cross-section $\frac{d\sigma}{dx_F}$ in order α_S^2 for the production of a charmed quark at $x_F = 2p_{\parallel}/\sqrt{S}$ at $\sqrt{S} = 62.4$ GeV. The total (solid curve) is comprised of the gluon gluon contribution (dashed curve) and the quark anti-quark contribution (dotted curve). The charmed quark mass is taken to be $m = 1.2$ GeV and the parton distributions DO2 were used.

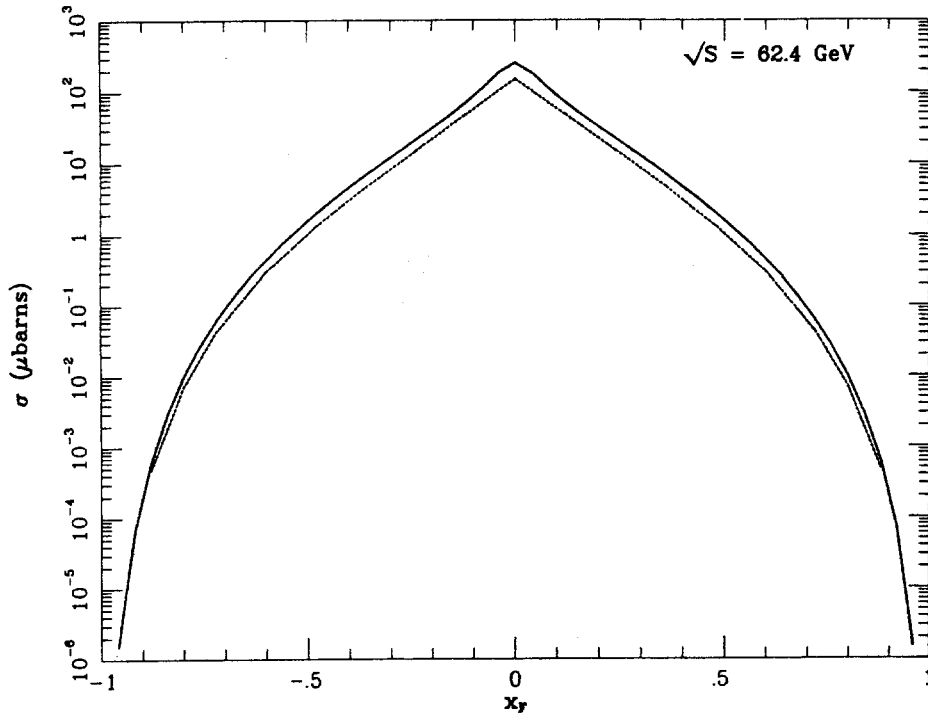


Figure 5: The differential cross-section $\frac{d\sigma}{dx_F}$ in order α_S^2 (solid curve) and including the order α_S^3 contribution from Eqs.(3.10, 3.19) (dotted curve). All other parameters as in Fig. 4.

scale of the hard interaction $\mu^2 = 4m^2$. After factorisation of the collinear singularities the resultant correction is always negative. Note that the quark-gluon contribution is expected to dominate only at large x_F and that that Fig. 5 is therefore expected to be reliable, including effects of order α_s^3 , only at large values of x_F . In the central region it is possible that the gluon gluon process Eq.(3.1B) makes a large modification of the lowest order prediction. Fig. 5 indicates that perturbative QCD effects do not give large modifications of the lowest order prediction in the forward region in proton nucleon scattering. This result is in stark contradiction with earlier work in ref. 6] where large modifications of the lowest order results were found from perturbative flavour excitation type contributions. We believe that the discrepancy is due to the fact that the authors of ref. 6] include pole terms ($1/t^2$) in the flavour excitation diagrams. Our complete gauge-invariant calculation shows that these terms are in fact cancelled.

It is amusing to note that process Eq.(1.3) introduces an asymmetry between the production of heavy quark or a heavy anti-quarks. Forming the combination,

$$C^{(-)}(p_1, p_2, p_3, p_4, p_5) = \frac{1}{2} [C(p_1, p_2, p_3, p_4, p_5) - C(p_1, p_2, p_4, p_3, p_5)] \quad (4.1)$$

we obtain in the same notation Eq.(3.12) as before,

$$\begin{aligned} C^{(-)}(p_1, p_2, p_3, p_4, p_5) = & \frac{N^2 - 4}{4N^2} \\ & \left[\frac{2}{t_{25}s_{34}} \left(\{23\}^2 + \{24\}^2 + \{35\}^2 + \{45\}^2 + \frac{m^2}{2}(t_{25} + s_{34}) \right) \right. \\ & \left(\frac{\{24\}}{\{12\}\{14\}} - \frac{\{23\}}{\{12\}\{13\}} + \frac{\{35\}}{\{13\}\{15\}} - \frac{\{45\}}{\{14\}\{15\}} \right) \\ & \left. + \frac{4m^2}{s_{34}t_{25}} \left(\frac{\{35\} + \{23\}}{\{14\}} - \frac{\{45\} + \{24\}}{\{13\}} \right) \right] \end{aligned} \quad (4.2)$$

In $p\bar{p}$ collisions at large values of the transverse momentum the processes of Eq.(3.1B,C) are expected to dominate. It could be that the mechanism of Eq.(4.2) induces an observable asymmetry between charmed and anti-charmed quarks in these processes.

Acknowledgments

I wish to acknowledge useful discussions with A.H. Mueller and C. Quigg. J. León collaborated with me during the early stages of this analysis. I am most grateful for his assistance.

References

1. A. Kernan and G. VanDalen, Phys. Rep. 106, 298 (1984).
2. J. L. Ritchie, Proc. 1984 Summer Study on the Design and Utilization of the SSC, R. Donaldson and J. Morfin, (eds.), APS (1984) and references therein.
3. R. K. Ellis, H. Georgi, M. Machacek, H. D. Politzer and G.G. Ross, Nucl. Phys. B152,(1979) 285 and references therein.
4. B. L. Combridge, Nucl. Phys. B151,(1979) 429.
5. P. Mazzanti and S. Wada, Phys. Rev. D26, (1982), 602.
6. V. Barger, F. Halzen and W. Y. Keung Phys. Rev. D25, 112 (1979).
7. S. J. Brodsky, P. Hoyer, C. Peterson and N. Sakai, Phys. Lett. 93B, (1980) 451;
S. J. Brodsky, C. Peterson and N. Sakai, Phys. Rev. D23, (1981) 2745.
8. P. D. B. Collins and T. P. Spiller, Durham Preprints DTP 84/4,84/22,84/26,84/40.
9. S. J. Brodsky and J. F. Gunion, Proc. 12th SLAC Summer Institute on Particle Physics, SLAC preprint SLAC-PUB-3527 (1984).
10. S. J. Brodsky, J. C. Collins, S.D. Ellis, J. F. Gunion and A. H. Mueller, Proc. 1984 Summer Study on the Design and Utilization of the SSC, R. Donaldson and J. Morfin, (eds.), APS (1984).
11. J. C. Collins, D. E. Soper, and G. Sterman, Nucl. Phys. B263,(1986) 37.
12. J. Babcock, D. Sivers and S. Wolfram, Phys. Rev D18,(1978) 162.
13. K. Hagiwara and T. Yoshino, Phys. Lett. 80B,(1979) 282;
L. M. Jones, and H. Wyld, Phys. Rev. D17,(1978) 782;
H. Georgi et al., Ann. Phys. 114,(1978) 273.
14. G. 't Hooft and M. Veltman, Nucl. Phys. B44,(1972) 189;
C. G. Bollini and J.J. Giambiagi, Nuovo Cim. 12B,(1972) 20;
W. J. Marciano, Phys. Rev. D12,(1975) 3861.
15. W. Furmański and R. Petronzio, Phys. Lett. 97B, (1980) 437, Z. Phys. C11, (1982) 293;
G. Curci, W. Furmański and R. Petronzio, Nucl. Phys. B175,(1980) 27.
16. E.G. Floratos, D. A. Ross and C. T. Sachrajda, Nucl. Phys. B129,(1977) 66, (E:B139,(1978) 545); Nucl. Phys. B152,(1979) 493.

17. A. Gonzalez-Arroyo, C. Lopez, and F. J. Yndurain, Nucl. Phys. B153,(1979) 161; Nucl. Phys. B159,(1979) 512.
18. A. H. Mueller and P. Nason, Columbia preprint, CU-TP-303, (1985).
19. F. Halzen and G. Herzog, Phys. Rev. D30, (1984) 2326;
F. Halzen and P. Hoyer, Phys. Lett. 154B, (1985) 324;
V. Barger and R. J. N. Phillips, Phys. Rev. D31, (1985) 215;
A. Ali and G. Ingelman, Phys. Lett. 156B, (1985) 111;
G. Kopp, J. H. Kuhn and P. Zerwas, CERN preprint CERN-TH-4081 (1984)
20. G. Altarelli and G. Parisi, Nucl. Phys. B126,(1977) 298.
21. F. A. Berends R. Kleiss, P. de Causmaecker, R. Gastmans and T. T. Wu, Phys. Lett. 103B, (1981) 102;
T. Gottschalk and D. Sivers, Phys. Rev. D21, (1980) 102.
22. Z. Kunszt and E. Pietarinen, Nucl. Phys. B164,(1980) 45.
23. M. Veltman, Schoonschip;
H. Strubbe, Comp. Phys. Comm. 8,(1974) 1.
24. W.A. Bardeen, A. Buras, D. W. Duke and T. Muta, Phys. Rev. D18, (1978) 3998.
25. D. W. Duke and J. F. Owens, Phys. Rev. D30, (1984) 49.
26. G. P. Lepage, J. Comput. Phys. 27, (1978) 192.